



Lyophobic Ordered Mesoporous Silica Additives for Li-O₂ Battery Cathode

Victor Roev, Sang Bok Ma, Dong Joon Lee and Dongmin Im*

Energy Lab., Samsung Advanced Institute of Technology, Samsung Electronics,
Electronic Materials Research Complex, 130 Samsung-ro, Suwon, 443-803, Korea

ABSTRACT

The surface of an ordered mesoporous silica (OMS) was functionalized using 1H,1H,2H,2H-perfluorooctyltrimethoxysilane at 20°C and 60°C. It was shown that only elevated temperature allows lyophobic properties on the walls of OMS, eventually preventing pore flooding with nonaqueous electrolytes. The functionalized OMSs (OMS-F) were characterized with various techniques: wettability test, N₂ sorption measurement, high-resolution transmission electron microscopy (HR-TEM). Cathodes of 10 mg/cm² loading were prepared with a commercial Pt/C catalyst and polyvinylidene fluoride (PVDF, 2.5 wt.%) binder using a typical doctor blade method on a commercial gas diffusion layer (GDL) in the presence or in the absence of OMS-F additives. Subsequent discharge-charge curves were taken in a 1M LiTFSI-TEGDME electrolyte at 60°C in pure oxygen atmosphere. It was found that the discharge capacity was significantly affected by OMS-F: 5 wt.% of additive extended discharge capacity by a factor 1.5. On the other hand, a similar OMS material but synthesized at 20°C did not show lyophobic properties and deteriorated cathode capacity.

Keywords : Li-air battery, oxygen transport, lyophobic ordered mesoporous silica, perfluorosilane

Received December 14, 2013 : Accepted December 31, 2013

Introduction

Li-air battery (or Li-O₂ battery more exactly) is a rising star in the electrochemical energy storage field. It is regarded as a promising alternative to the well developed lithium ion batteries due to its very high theoretical energy density [1-4]. Nonetheless, the combination of scientific and technological challenges does not allow fast breakthrough of Li-air batteries into the market and postpones commercialization [5,6]. One of the main challenges in the development of practical rechargeable Li-air battery is the design and the development of a highly

efficient cathode viable in oxidative environment. The field of cathode development has been actively involved in searching for new electrode materials of better stability [7,8], additives for improving the charging behavior [9,10], lithium salts with anions having good electron delocalization and stability in the cathode environment [11], and new nonaqueous solvents with optimal combination of chemical and electrochemical stability, low volatility, low mobility inside cathode as well as good compatibility with electrode materials [12,13]. In principle, an ideal cathode material for nonaqueous Li-air battery should possess several critical properties including

*Corresponding author. Tel.: +82-31-8061-1233

E-mail address: dongmin.im@samsung.com

Open Access DOI: <http://dx.doi.org/10.5229/JECST.2014.5.2.58>

This is an Open Access article distributed under the terms of the Creative Commons Attribution Non-Commercial License (<http://creativecommons.org/licenses/by-nc/3.0/>) which permits unrestricted non-commercial use, distribution, and reproduction in any medium, provided the original work is properly cited.

(1) high electrical conductivity for fast electrons transfer, (2) optimized pore structure to accommodate a large amount of discharge products, (3) rapid transportation of lithium ions and oxygen, (4) high selectivity for catalyzing lithium peroxide formation/oxidation, (5) chemical, electrochemical, and structural stability, and (6) compatibility with electrolytes.

According to the critical analysis given by an automaker, one of the most challenging aspects for practical Li-air battery is the necessity of very high areal capacity (*ca.* >40 mAh/cm²), which represents an order of magnitude increase over the state-of-the-art research cells [14]. To satisfy this requirement a cathode with high loading level appears to be indispensable. On the other hand, it has been found that the oxygen transport into the carbon cathode through the electrolyte has a direct impact on the discharge capacity [15,16] and may be sluggish in the case of thick cathode. Meanwhile, the oxygen solubility and the oxygen diffusion control this transport that eventually has a direct effect on the distribution of discharge product inside the cathode. For instance, the raised oxygen transport resistance is significant when the volume fraction of insoluble discharge products is more than 50 vol.% [17]. Various approaches to increase the specific capacity of cathode and the energy density of Li-O₂ batteries have been studied. A drift-diffusion-based model predicts that partially flooded cathodes and/or non-uniform catalyst distribution may increase the energy density of Li-O₂ batteries [18]. Another approach to increase specific discharge capacity is the modification of carbon surface with long-chain hydrophobic molecules [19], in which the authors conclude that such kind of modification mitigates carbon surface passivation due to the formation of more conductive and less dense Li oxide layer. Unfortunately, enough attention has not been paid to the difference between partially or fully flooded state of the cathode although it has already been demonstrated that air electrode design has a great influence on the discharge capacity achieved [20]. Indeed, silane-based hydrophobic coating on a carbon gas diffusion layer (GDL) greatly enhances specific capacity in comparison with Al-grid and nickel foam substrates. There has been a consensus that the creation of desirable 3-phase percolation throughout the air electrode (or enabling continuous gas-diffusion paths) is mandatory for effective cathode operation in Li-O₂ batteries [20-22].

In this work, we have developed a strategy com-

paring lyophobic fluorinated porous silica additive with highly active electrocatalyst to fabricate a thick cathode, which endows a stable dual pore system. Furthermore, we show that a thick Pt/C based cathode of 10 mg/cm² loading containing 5 wt.% lyophobic OMS can deliver a very high specific capacity even in fully flooded conditions.

2. Experimental

2.1 Chemicals and materials

Following chemicals and materials were purchased and used as received without additional purification: acetone (99%, Sigma-Aldrich, USA), (1H,1H,2H,2H-Perfluorooctyltrimethoxysilane (97%, #S13160, Fluorochem., UK), hexamethylacetone (98%, Sigma-Aldrich, USA), N-methylpyrrolidone (98%, Sigma-Aldrich, USA), lithium bis-(trifluoromethanesulfonyl)imide (LiTFSI) (PANAX ETEC Co., Korea), propylene carbonate (PC) (battery grade, PANAX ETEC Co., Korea), tetraethylene glycol dimethyl ether (TEGDME) (anhydrous, Sigma-Aldrich, USA), ordered mesoporous silica (*d* = ~10 nm, S-Chemtech Co. Ltd, Korea), 28 wt.% Pt/C electrocatalyst (TEC36V52, TKK, Japan), polyvinylidene fluoride (PVDF) (#5130, Solvay Co., Belgium), and gas diffusion layer SGL 25BC (SGL Technologies GmbH., Germany). A lithium conductive glass-ceramic membrane (250 μm thick, LATP, Ohara Glass Co., Japan) was applied as separator to protect lithium metal anode from oxygen and moisture. A microporous separator film (Celgard 3501, 25 μm thick) was placed between anode and the glass-ceramic membrane. Nickel terminal foil and aluminum laminated pouch were supplied from Samsung SDI.

2.2. OMS-F synthesis

1 mL of 1H,1H,2H,2H-perfluorooctyltrimethoxysilane was added into 4 mL of hexamethylacetone and the resulting solution was stirred vigorously for 1 min. Then, the solution was mixed with 1 g of OMS inside a zipped plastic bag for 15 min. The plastic bag was immersed into a 1 L stainless steel container and tightly sealed. The container was kept at 20°C or 60°C for 48 h, then opened. The powder thus obtained was dried in a convection oven at 80°C for 24 h then followed by a vacuum drying at 120°C for 12 h.

2.3. Preparation of OMS-F and Pt/C blend

Usually a blend of OMS-F and Pt/C were prepared before the electrode fabrication. For example, 5 wt.% OMS-F and Pt/C blend was prepared with the following procedure: 0.95 g of Pt/C (28 wt.% Pt, TKK) catalyst was ultrasonically dispersed in 200 mL of deionized water for 15 min using a Sonopuls ultrasonic homogenizer (power: 20%, duty cycle: 50%, titanium horn), then the resulting suspension was mixed with 0.05 g of OMS-F soaked with 20 mL of acetone and ultrasonically treated again in a similar way for 15 min. The product was washed with deionized water 3~4 times and dried in a freeze dryer.

2.4. Electrode fabrication, Li-O₂ cell preparation and testing

All cathodes comprised the Pt/C electrocatalyst with or without OMS-F. The electrocatalyst was mixed with 5 wt.% PVDF dissolved in N-methylpyrrolidone for 30 min at 1000 rpm in a mixer (Thinky ARE-250). The slurry thus prepared was applied on a SGL 25BC gas diffusion layer using a doctor blade method, and then dried in two steps (at 25°C for 24 h, then at 120°C for 2 h). Circular electrodes of 0.5 cm² area were cut out for the cell assembly and each one contained around 10 mg/cm² of dried electrocatalyst (Pt/C, binder, and OMS-F combined). To avoid the influence of anode on the electrochemical behavior of cathode, the protected lithium anode was fabricated in advance. A Li foil of 500 μm thickness and 2 cm² area was laminated with a nickel foil current collector. The protected lithium anode was assembled by laminating lithium metal, a Celgard 3501 separator fully soaked with a nonaqueous electrolyte (1.0 M LiTFSI in PC), and the LAMP glass-ceramic membrane in a plastic package, leaving a rectangular window of 1.2 cm² open to the cathode side. Stainless steel mesh was used as the cathodic current collector. The electrolyte for the cathode was 1.0 M LiTFSI in TEGDME. After finishing the assembly, the Li-O₂ cell was placed in a 1 L container as schematically shown in Fig. 1. The container was purged with oxygen gas for 30 min and finally sealed hermetically. The oxygen pressure of about 1 atm and the temperature of 60°C were maintained during the electrochemical tests. The Li-O₂ cells were discharged from open circuit potential (OCP) to 2.0 V, then charged up to 4.0 V at a current density of 1 mA/cm² by means of a Toyo multi-channel battery cycler (Japan).

2.5. Characterization

Transmission electron microscopy (TEM) images were obtained using a TECNAI FE-20 microscope (FEI Co.) at an accelerating voltage of 200 kV. Pore characteristics were measured by taking N₂ adsorption-desorption isotherms (Tristar 3000, Micromeritics, USA). Brunauer-Emmett-Teller (BET) and Barrett-Joyner-Halenda (BJH) methods were used to estimate the surface area and the pore size distributions, respectively. The estimation of micropores and external surface area were accomplished using a t-plot method. Prior to the measurements, all samples were completely dried under vacuum at 120°C for 12 h. Thermogravimetric analysis (TGA) was carried out with a Mettler Toledo TGA1 instrument in an aluminum pan with heating rate of 5°C per minute in air. Wettability assessment experiments were performed as follows: a droplet of cathodic electrolyte (about 1 mL) was placed on a clean glass surface and then a

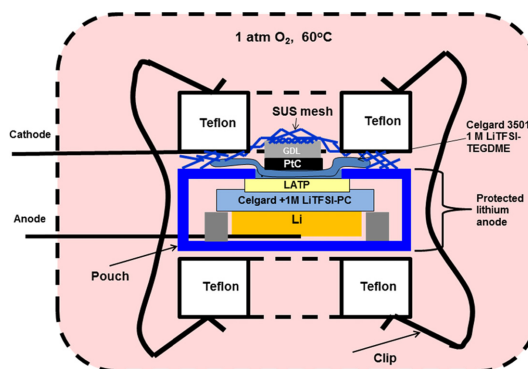


Fig. 1. Schematic view of the nonaqueous Li-O₂ cell used in this study comprising protected lithium anode and placed in a sealed container.

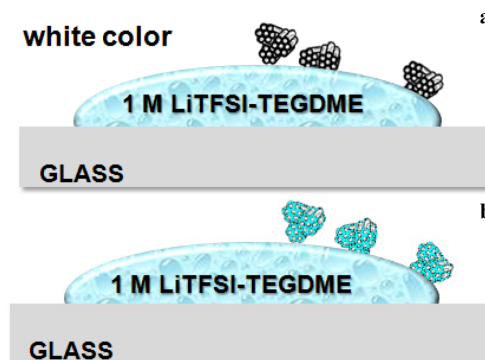


Fig. 2. Illustrations of OMS wettability test representing (a) lyophobic surface and (b) wettable surface.

few milligrams of the OMS powder of interest were applied on the electrolyte surface. When the OMS surface is soaked with electrolyte, the color of powder immediately turns transparent due to the electrolyte adsorption. On the other hand, when the surface of OMS is lyophobic enough, the white color is not changed and the particles are floating on the liquid surface for a long time. Schematically this procedure is shown in Fig. 2.

3. Results and discussion

It is reasonable to assume that the cathode of high loading level can supply more surface sites for lithium peroxide formation to ensure high areal capacity. It has also been mentioned above that the efficient cathode design must account for the non-uniform accommodation of the substantial amounts of discharge product in whole cathode volume. To improve this, we suggest a special cathode design, which is schematically presented in Fig. 3. We speculate that a proper OMS additive having lyophobic inner pore surfaces may provide sustainable air channels and enhance O_2 transport inside of thick cathode even under flooded electrolyte conditions.

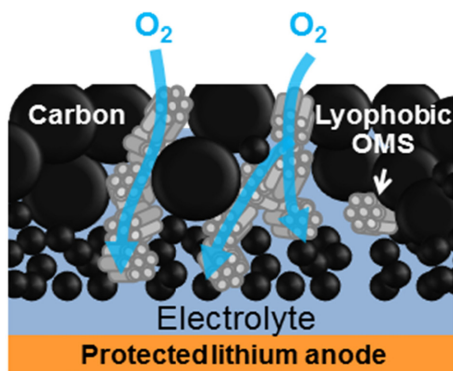


Fig. 3. Conceptual illustration of the lyophobic pore effect with improved cathode design.

As an effort to fabricate sustainable dual-pore cathodes with good structural integrity, a few well-established or commercially available OMSs have been evaluated in terms of their pore characteristics and particle size. Summarized results are presented in Table 1. KIT-6 and MCM-48 prepared with standard procedures [23,24] consist of large particles or aggregates, which make it difficult their uniform distribution with other carbon particles inside the cathode. In fact, only the OMS sample supplied from S-Chemtech (for simplicity we call it OMS from this point) shows relatively small primary particle size allowing its incorporation into the cathode layer (Fig. 4a). In addition to the proper particle size characteristics, it also reveals a large pore size (Fig. 4b). The large mesopore (~10 nm) might provide enough space not only for the surface functionalization of the inner wall of pores but also for the accommodation of discharge products.

Indeed, the HR-TEM images reveal that the OMS sample demonstrates a honeycomb-like pore structure and the estimated pore size is about 7.1 nm, correlating very well with that measured with N_2 desorption isotherm (8.2 nm, inset of Fig. 4c). It should be noted that the average pore size of OMS for the whole measured range is listed in Table 1 and it is slightly larger than discussed above.

It is well known that silane compounds can easily be immobilized on the surface of silica and it can be modified to be highly lyophobic with the use of perfluorosilane. We believe the lyophobicity and the chemical inertness of perfluorocompounds might contribute to the improvement of Li- O_2 battery technology.

All functionalized silica samples have been prepared and analyzed in a similar manner. The TGA data allow the estimation of perfluorosilane loading on the silica surface. Fig. 5 shows the weight losses upon a slow heating in air. The pristine silica samples show quite stable behavior over all temperature range, but the treated samples show a few characteristic regions. In the early stage of heating between 30 and 150°C, no significant weight

Table 1. Pore characteristics of some selected OMSs

OMS	particle size, μm	BET surface area, m^2/g	t-plot external surface area, m^2/g	surface area corresponding to 1.7- 300 nm pores, cm^3/g	average pore size, nm
MCM-48	>1.0	1085	1084	1.07	2.9
KIT-6	1-50	532	431	0.57	4.8
OMS (S-Chemtech)	0.1	621	563	1.62	10.1

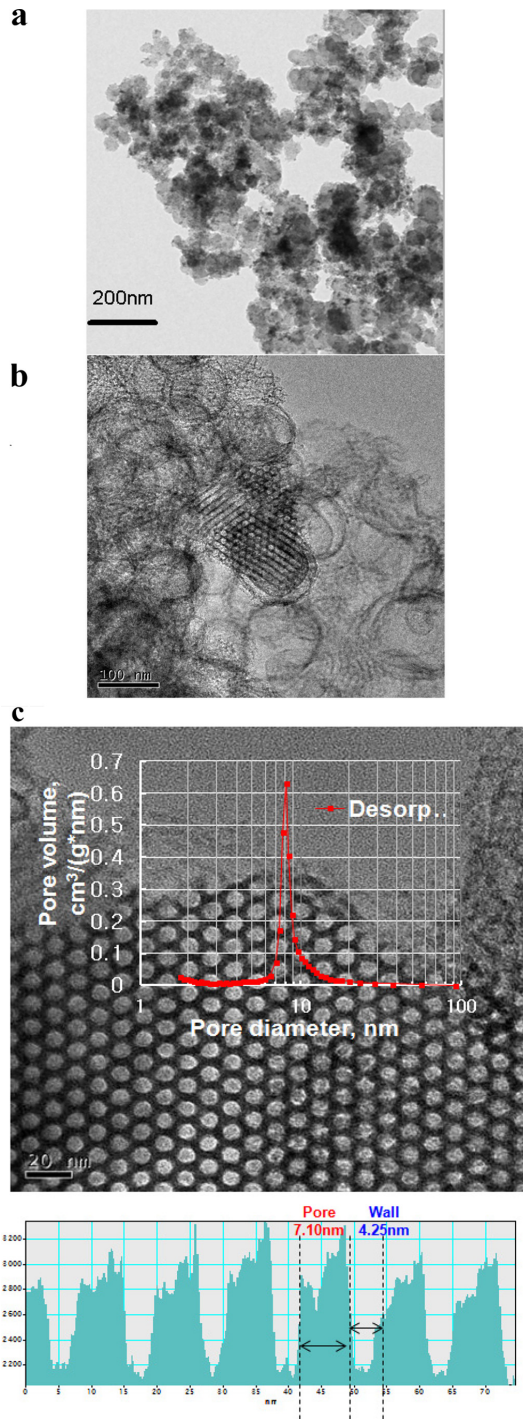


Fig. 4. Pt/C and OMS characterization results: (a) a TEM photograph of Pt/C material used in this study, (b) a TEM photograph of OMS supplied from S-Chemtech, and (c) a BJH desorption characteristics of OMS imposed on a TEM photograph.

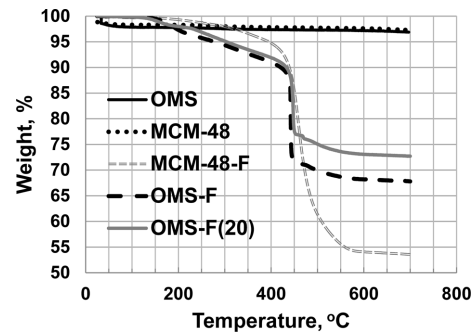


Fig. 5. TGA results of various porous silica materials performed in air at a heating rate of 5°C/min.

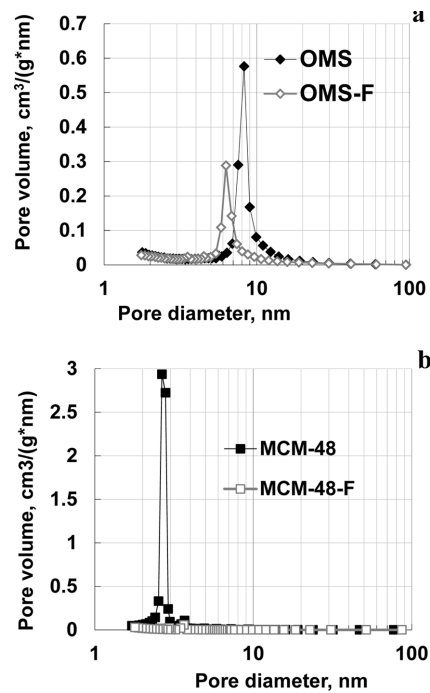


Fig. 6. Pore size distribution curves obtained with a BJH method representing the OMS samples before and after functionalization: (a) OMS from S-Chemtech and (b) MCM-48.

loss is found. Then a sluggish weight loss region (~10%) between 150 and 445°C is followed. Finally a significant loss near 445°C can be easily recognized. This kind of behavior is very similar to the polydimethylsiloxane treated silica heated in nitrogen atmosphere [25]. We can assume that C-C bond cleavage may begin already at 44°C due to its relatively small dissociation energy (~300 kJ/mol) in comparison with other chemical bonds, such as Si-C (435 kJ/mol) and Si-O (798 kJ/mol)

[26,27]. TGA curves also provide the data on the fraction of the organic material burned or thermally decomposed by the end of measurement. The functionalized OMS synthesized at 60°C is found to have 32.2 wt.% of perfluorosilane and is now denoted as OMS-F. The functionalized silica prepared similarly, but synthesized at 20°C (denoted as OMS-F(20)) contains 27 wt.% perfluorosilane, indicating that even relatively low synthesis temperature (20°C) allows silica to be functionalized. It is not surprising that MCM-48 of large surface area demonstrates the highest perfluorosilane loading (46.5 wt.%).

We have extended material characterization by taking N₂ sorption measurements. Fig. 6 shows that the pore characteristics of porous silica samples are dramatically changed after functionalization. OMS-F still shows narrow open pores around 6.5 nm that will be able to provide fast gas transport, but the pores of MCM-48-F are completely blocked and cannot be considered as a mesoporous material any more.

To further understand which OMS will be best additive to the Pt/C-based cathodes, the wettability of functionalized silica samples has been examined. Table 2 summarizes the results of wettability test for a few selected materials. It is found that the wetting behavior of the functionalized materials with electrolyte is completely different from that of pristine ones. As we have anticipated the pristine porous silicas can be easily soaked with our aprotic electrolyte (1.0 M LiTFSI in TEGDME). The large surface area and the oxygenative functional groups on silica appear to

Table 2. Wettability assessment results of a few selected mesoporous materials

Material	Conditions and Composition	Wetting Behavior	Conclusion
OMS	no treatment	Instantaneous	No electrolyte-proof effect
OMS-F(20)	20°C treated	Very fast	
MCM-48	no treatment	Instantaneous	Electrolyte-proof surface
MCM-48-F	no open mesopores, 60°C treated, 46.5 wt.% perfluorosilane	No	
OMS-F	6.5 nm, 60°C treated, 32.2 wt.% perfluorosilane		

favor intermolecular interactions between electrolyte and solid, eventually leading to the instantaneous wetting. In addition, capillary forces might also enhance the wettability of porous materials.

OMS-F(20) sample treated at a low temperature does not show any electrolyte-proof properties, meaning that some hydroxyl groups are still exposed on the silica surface even after vacuum drying. In sharp contrast, other functionalized mesoporous silica samples (OMS-F and OMCM-48-F) show pronounced electrolyte-proofing effect and can be recommended as additives for the cathode modification.

To prove our concept and further examine the behavior of OMS inside the cathode comprising electrocatalyst materials, the following electrochemical experiments have been performed. The Pt/C-based cathodes have been prepared as described in Experimental section with and without the addition of porous silica samples. Li-O₂ cell has been constructed with each cathode (Fig. 1) and the initial discharge capacity of each cell is presented in Table 3 and some selected voltage profiles are shown in Fig. 7.

Table 3. Initial discharge capacities of Pt/C cathodes with and without OMS-F additives

Additive	Capacity, mAh/g _{cathode}
none	541
2.5 wt.% OMS-F(20)	435
8 wt.% OMS-F(20)	360
5 wt.% MCM-48-F	532
2.5 wt.% OMS-F	535
5 wt.% OMS-F	828
8 wt.% OMS-F	713

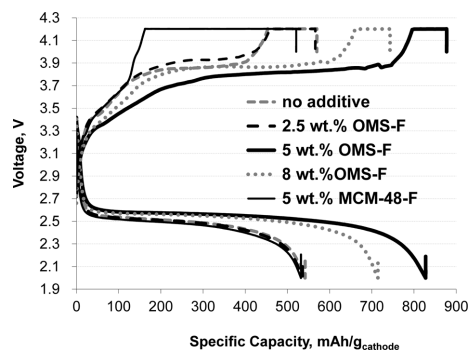


Fig. 7. Initial discharge and charge profiles of selected Li-O₂ cells.

It is found that even small amount of OMS-F(20) deteriorates the discharge capacity. We speculate that the capacity decrease after the cathode modification is ascribed to the decrease of electrical conductivity originating from the insulating properties of OMS additives and/or more pronounced cathode flooding, retarding the oxygen transport and leading to non-uniform reaction zones. On the other hand, in similar experiments carried out with highly lyophobic OMS-F as additives, the improvement of discharge capacity can be observed (Fig. 7) even though the addition of OMS-F might have reduced the electrical conductivity of cathodes. It leads us to the conclusion that this difference is associated with the oxygen transport properties, not the electrical conductivity. These experimental results also suggest that the modified Pt/C-based cathode can tailor the oxygen transport behavior and improves the volume utilization, consequently improving the specific discharge capacity of Li-O₂ battery by a factor 1.5. However, the cathode modification does not significantly affect the charge and discharge voltages, indicating it probably does not change discharge/charge mechanism. The data presented in Table 3 also show a qualitative evidence suggesting that the cathode flooding is an important issue and should be overcome in practical Li-O₂ batteries.

4. Conclusions

In summary, the lyophobic mesoporous silica synthesized at an elevated temperature has been investigated as an additive for the Pt/C based cathode in a Li-O₂ battery equipped with protected lithium anode. It is shown that the addition of 5 wt.% of lyophobic porous silica to the cathode enhances the specific discharge capacity by a factor of 1.5 in a TEGDME-based electrolyte. The improvement is attributed to its improved oxygen transport properties, which are vital to the operation of Li-O₂ battery cathodes, including open porous structure and highly lyophobic character of pores. It is also demonstrated that a similar additive synthesized at 20°C does not show lyophobic properties, eventually deteriorating the cathode performance. We hope that our results would encourage further detailed investigation of cathode for overcoming many challenges for practical Li-O₂ batteries.

References

- [1] P.G. Bruce, S.A. Freunberger, L.J. Hardwick and J.M. Tarascon, *Nat. Mater.*, **11**, 19 (2012).
- [2] H.G. Jung, H. G. J. Hassoun, J.B. Park, Y.K. Sun and B. Scrosati, *Nat. Chem.*, **4**, 579 (2012).
- [3] Z. Peng, S.A. Freunberger, Y. Chen and P.G. Bruce, *Science*, **337**, 563 (2012).
- [4] T. Zhang, and H. Zhou, *Nat. Commun.* **4**, 1817 (2013).
- [5] G. Girishkumar, B. McCloskey, A.C. Luntz, S. Swanson and W. Wilcke, *J. Phys. Chem. Lett.* **1**, 2193 (2010).
- [6] J. Christensen, P. Albertus, R.S. Sanchez-Carrera, T. Lohmann, B. Kozinsky, R. Liedtke, J. Ahmed and A. Kojic, *J. Electrochem. Soc.*, **159**, R1 (2012).
- [7] S.H. Oh, R. Black, E. Pomerantseva, J.-H. Lee and L.F. Nazar, *Nat. Chem.*, **4**, 1004 (2012).
- [8] M.M.O. Thotiyl, S.A. Freunberger, Z. Peng, Y. Chen, Z. Liu and P.G. Bruce, *Nat. Mater.*, **12**, 1050 (2013).
- [9] Y. Chen, S.A. Freunberger, Z.Peng, O. Fontaine and P.G. Bruce, *Nat. Chem.*, **5**, 489 (2013).
- [10] M.J. Lacey, J.T. Frith and J.R. Owen, *Electrochem. Commun.*, **26**, 74 (2013).
- [11] G.M. Veith, J. Nanda, L.H. Delmau and N.J. Dudney, *J. Phys. Chem. Lett.*, **3**, 1242 (2012).
- [12] V.S. Bryantsev, J. Uddin, V.Giordani, W. Walker, D. Addison and G.V. Chase, *J. Electrochem. Soc.*, **160**, A160 (2013)
- [13] C.O. Laoire, S. Mukerjee, K.M. Abraham, E.J. Plichta and M.A. Hendrickson, *J. Phys. Chem. C*, **114**, 9178 (2010).
- [14] J. Adams and M. Karulkar, *J. Power Sources*, **199**, 247 (2012)
- [15] J. Read, *J. Electrochem. Soc.*, **149**, A1190 (2002).
- [16] J. Read, *J. Electrochem. Soc.*, **153**, A96 (2006).
- [17] Y. Wang and S.C. Cho, *J. Electrochem. Soc.*, **160**, A1847 (2013).
- [18] P. Andrei, J.P. Zheng, M.A. Hendrickson and E.J. Plichta, *J. Electrochem. Soc.*, **157**, A1287 (2010).
- [19] C. Tran, J. Kafle, X.Q. Yang and D. Qu, *Carbon*, **49**, 1266 (2011).
- [20] J. Christensen, P., R. S. Sanchez-Carrera, T.Lohmann, B. Kozinsky, R. Liedtke, J. Ahmed and A. Kojic, *J. Electrochem. Soc.*, **159**, R1 (2012).
- [21] R.E. Williford, J. Zhang, *J. Power Sources*, **194**, 1164 (2009).
- [22] J. Xiao, W. Xu, D. Wang and Ji-G Zhang, *J. Electrochem. Soc.*, **157**, A294 (2010).
- [23] J.M. Kim, S.K. Kim and R. Ryoo, *Chem. Commun.*, 259 (1998).
- [24] C. Jo, K. Kim and R. Ryoo, *Micropor. Mesopor. Mater.*, **124**, 45 (2009).
- [25] A.L. Lopes and F. Augusto, *J. Chromatogr. A*, **1056**, 13 (2004).
- [26] T. L. Cottrell, *The Strengths of Chemical Bonds*, 2nd Ed., Butterworth, London (1958).
- [27] B. deB. Darwent, *National Standard Reference Data Series*, National Bureau of Standards, N31, Washington (1970).